

FPSAttention: Training-Aware FP8 and Sparsity Co-Design for Fast Video Diffusion

Akide Liu^{*1,2,3}, Zeyu Zhang^{*2}, Zhexin Li^{†2,4}, Xuehai Bai^{†3}, Yizeng Han², Jiasheng Tang^{‡24}, Yuanjie Xing², Jichao Wu^{2,4}, Mingyang Yang^{2,4}, Weihua Chen², Jiahao He³, Yuanyu He³, Fan Wang², Gholamreza Haffari¹, Bohan Zhuang^{‡2,3}

¹Monash University ²DAMO Academy, Alibaba Group ³ZIP Lab, Zhejiang University ⁴Hupan Lab
^{*}Co-first authors, [†]Co-second authors, [‡]Project leads, Details see Sec.6.

Diffusion generative models have become the standard for producing high-quality, coherent video content, yet their slow inference speeds and high computational demands hinder practical deployment. Although both quantization and sparsity can independently accelerate inference while maintaining generation quality, naively combining these techniques in existing training-free approaches leads to significant performance degradation, as they fail to achieve proper joint optimization. We introduce **FPSAttention**, a novel training-aware co-design of FP8 quantization and Sparsity for video generation, with a focus on the 3D bi-directional attention mechanism. Our approach features three key innovations: 1) A unified 3D tile-wise granularity that simultaneously supports both quantization and sparsity. 2) A denoising step-aware strategy that adapts to the noise schedule, addressing the strong correlation between quantization/sparsity errors and denoising steps. 3) A native, hardware-friendly kernel that leverages FlashAttention and is implemented with optimized Hopper architecture features, enabling highly efficient execution. Trained on Wan2.1’s 1.3B and 14B models and evaluated on the VBench benchmark, **FPSAttention** achieves a 7.09× kernel speedup for attention operations and a 4.96× end-to-end speedup for video generation compared to the BF16 baseline at 720p resolution—without sacrificing generation quality.

Date: June 10, 2025

Project page and code: <https://fps.ziplab.co>

Correspondence: fan.w@alibaba-inc.com, bohan.zhuang@gmail.com



arXiv:2506.04648v2 [cs.CV] 6 Jun 2025

1 Introduction

Diffusion models have revolutionized AI through breakthrough image synthesis [41, 7, 36] and are advancing into complex video generation [42, 47]. Diffusion Transformers (DiTs) [29] now enable efficient, high-quality synthesis [1, 24], powering billion-parameter models like Wan2.1 [39] that produce coherent, long-duration, high-fidelity videos.

Despite progress, crippling computational demands persist [34]: (i) iterative reverse-diffusion requiring hundreds of steps, and (ii) quadratic-complexity spatio-temporal attention ($\mathcal{O}(N^2)$, N denotes the number of tokens) [23, 18, 39]. Particularly, the computational burden of attention becomes prohibitive for high-resolution, long-duration videos, often consuming >70% of inference time [54, 45, 37]. For instance, Wan2.1-14B requires approximately 2.5 hours on an NVIDIA H20 GPU to generate a 5s video.

To address the efficiency challenge, numerous acceleration methodologies have been proposed [8, 25, 35], among which quantization and sparsity have emerged as predominant techniques [40, 26]. Quantization reduces numerical precision (e.g., FP32→INT8/FP8), thereby decreasing the memory footprint and enabling faster computations (Figure 1 (a)). The recent post-training quantization (PTQ) method SageAttention [52] quantizes attention modules into

Method	Kernel Speedup	E2E Speedup
BF16	1.00×	1.00×
FP8	1.84×	1.26×
STA	5.15×	3.60×
FPSAtten	7.09×	4.96×

Table 1 Efficiency comparison of the BF16 baseline, FP8 quantization, STA sparse attention, and our **FPSAttention** on Wan2.1-14B at 720p resolution on an NVIDIA H20 GPU. We report both kernel-level and end-to-end speedups relative to the BF16 baseline.

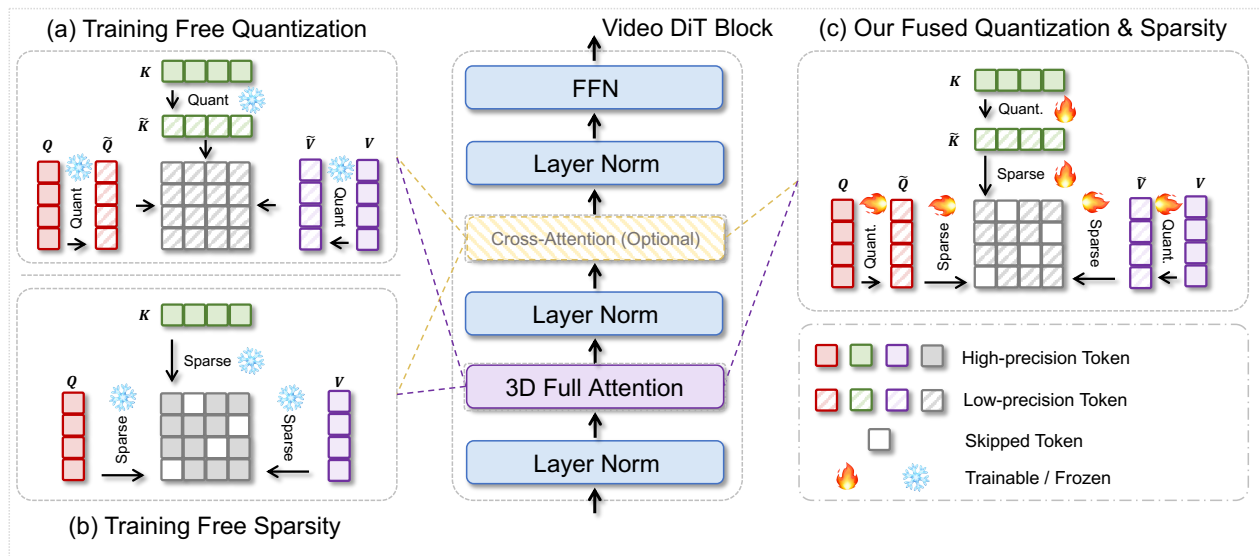


Figure 1 Comparing previous training-free quantization (a) and training-free sparsity (b) approaches reveals substantial accuracy degradation and a lack of compatibility when used independently. In contrast, our **FPSAttention** framework (c) integrates low-precision and sparse patterns in a single training process, yielding near-zero accuracy loss and seamless deployment.

INT8 with calibration strategies, providing moderate acceleration with downgraded generation quality. Compared to INT8, the emerging format FP8 quantization offers a wider dynamic range[27], facilitating both training and inference [19, 33]. Nevertheless, training-free FP8 quantization, despite its theoretical advantages, introduces significant quantization errors that degrade model performance [52]. Apart from quantization, sparsity techniques address the quadratic computational complexity of 3D full attention by selectively skipping computations, as illustrated in Figure 1 (b). Representatively, Sparse-VideoGen [45] implements per-head spatial-temporal masks aligned with GPU blocks, SpargeAttn [53] employs a two-stage filtering mechanism, and Sliding Tile Attention (STA) [54] leverages local 3D sliding windows with kernel-level optimizations.

To enjoy the benefits of both worlds, a straightforward strategy is jointly applying FP8 quantization and sparsity. However, a naive combination presents significant challenges, as quantization errors can be magnified when combined with sparsity mechanisms [46], as shown in Figure 2. Intuitively, sparsity techniques prioritize token retention with high-magnitude attention scores, while quantization disproportionately introduces errors in these high-magnitude values. This intrinsic tension necessitates holistic approaches that consider both techniques simultaneously, potentially framing sparsification as a specialized form of 0-bit quantization to achieve optimal balance between efficiency and generation quality [28].

Furthermore, existing approaches largely overlook training-aware joint optimization of quantization and sparsity, creating a substantial training-inference gap. Our empirical analysis (Section 3.3) reveals that diffusion models can tolerate and even correct for hardware-friendly tile-wise errors. The error resilience is particularly pronounced when the model is aware of approximations via quantization-aware training (QAT), ensuring consistent performance at inference time.

In this paper, we introduce **FPSAttention**, as shown in Figure 1(c), a novel training-aware co-design framework that synergistically integrates FP8 quantization and structured sparsity for 3D attention in video DiTs.

Figure 2 Comparison of video generation results. Top: Training Free FP8 + STA. Bottom: Our Training-Aware **FPSAttention**. Click the image to play the video via Acrobat Reader.

FPSAttention proposes three key innovations:

- *Unifying Tile-wise Operations*: Implementing a 3D tile-wise granularity for both FP8 quantization and block sparsity (section 3.2), which directly aligns with efficient hardware execution patterns (e.g., GPU Tensor Cores) and forms the basis for structured acceleration.
- *Denoising Step-Aware Scheduling*: Introducing an adaptive strategy (section 3.3) that dynamically adjusts quantization and sparsity granularity according to the varying error sensitivity and corrective capacity of the model across different denoising timesteps.
- *Hardware-Optimized Kernel Design*: Developing a native, high-performance kernel (section 3.4) leveraging features like FlashAttention and NVIDIA Hopper architecture optimizations to translate theoretical FLOPs reduction into tangible wall-clock speedups.

As demonstrated in Table 1, by training on Wan2.1’s 1.3B and 14B models and evaluating on the vBench benchmark, FPSAttention achieves a **7.09** \times kernel speedup for attention operations and a **4.96** \times end-to-end speedup for video generation compared to the BF16 baseline, all without sacrificing generation quality, significantly outperforming approaches that apply quantization (1.84 \times kernel speedup) or sparsity (5.15 \times kernel speedup) independently. Our work not only provides a practical solution for accelerating video diffusion but also offers a new perspective on the robustness of diffusion models to aggressive, structured compression.

2 Related Work

Quantization for video generation models. The computational expense of video generation models, particularly Diffusion Transformers (DiTs) [18], driven by iterative sampling [12] and quadratic attention complexity [37], necessitates model quantization techniques [34]. Post-Training Quantization (PTQ) has been explored for its efficiency [11, 21, 14, 3, 16]; however, applying PTQ to video DiTs presents unique challenges beyond standard image models [44, 4, 56]. Temporal variability of activation statistics across denoising steps [15] has prompted PTQ methodologies to implement time-step-wise calibration [48], adaptive quantization, and dynamic smoothing techniques [32]. Recent work has evaluated these techniques on standardized benchmarks (e.g., VBench [17]), assessing temporal consistency alongside perceptual quality. While PTQ approaches show promising results, Quantization-Aware Training (QAT) for video diffusion models remains largely unexplored. Our work addresses this gap by introducing an FP8 QAT framework that jointly optimizes quantization and sparsity, enabling efficient video generation while maintaining visual fidelity.

Sparse attention for video generation models. Recent advancements in sparse video generation and efficient attention mechanisms have improved memory utilization and computational efficiency. Sparse VideoGen [45] leverages sparsely sampled motion priors to produce realistic videos while reducing temporal redundancy. Efficient attention mechanisms have proven crucial for handling long-range dependencies in video data. Sliding Tile Attention [54] introduces a tiled sparse attention mechanism for modeling spatial-temporal correlations, while SpargeAttn [53] proposes progressive sparsification by selectively pruning attention tokens based on importance scores. DiTFastAttn [2] accelerates attention computation by dynamically filtering irrelevant patches, achieving significant speedups without compromising quality. These approaches illustrate the trend of combining structured sparsity with content-aware selection for scalable video generation. However, these methods are typically limited to inference-time acceleration, lack integration with model training procedures, and are not fully compatible with quantization techniques, creating challenges for developing holistically efficient video generation frameworks.

3 Method

Our technique integrates algorithmic innovation with hardware-conscious kernel optimization to enhance the efficiency of video DiTs. This section begins by establishing fundamental concepts essential to our methodology. Subsequently, we introduce the architecture of our proposed FPSAttention, detailing its two primary algorithmic contributions: a unified tile-wise quantization and sparse attention mechanism, and a denoising step-aware strategy for dynamic adaptation of quantization and sparsity hyperparameters. Finally,

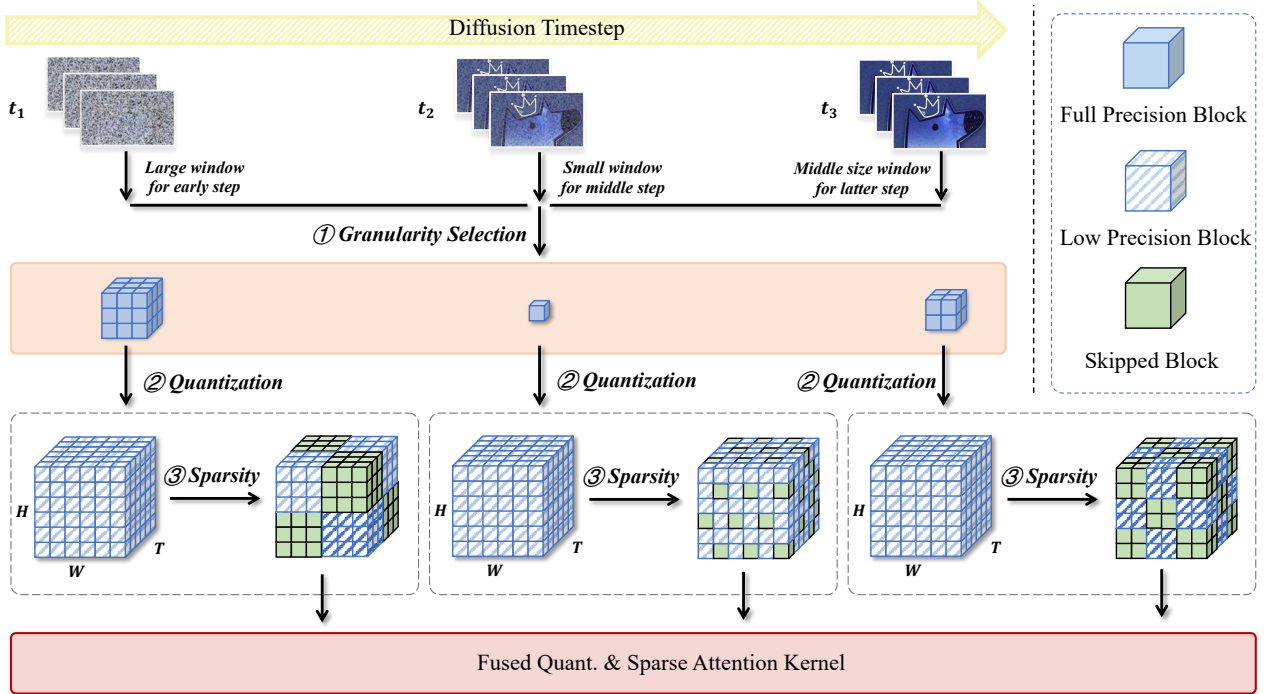


Figure 3 Overview of FPSAttention. (1) Our approach synergistically optimizes joint quantization and sparsity patterns within the attention mechanism for efficient video generation. (2) We introduce a novel denoising step-aware strategy that dynamically adapts the granularity throughout the diffusion process, balancing computational efficiency and perceptual fidelity. Empirical observations are shown in Figure 5. (3) A fused hardware-friendly kernel is applied for attention operations.

we outline our hardware-optimized kernel implementation that plays a crucial role in translating theoretical computational savings into practical efficiency gains. Figure 3 provides a high-level conceptual overview of our FPSAttention framework.

3.1 Background

This subsection establishes the two foundational techniques that underpin our methodology: 8-bit floating-point (FP8) quantization and Sliding Tile Attention (STA).

FP8 quantization. Video Diffusion Transformers (DiTs) process $L = T \times H \times W$ spatiotemporal tokens, where T , H , and W represent temporal frames, height, and width dimensions. To reduce memory bandwidth requirements for activation tensors, FP8 quantization approximates each value $X_{i,j}$ using an 8-bit floating-point representation. Unlike INT8 quantization, which maps continuous values to a scaled integer grid, FP8 conversion preserves the floating-point nature by utilizing dedicated sign, exponent, and mantissa bits (in formats such as E4M3 or E5M2).

The FP8 conversion employs a scaling factor s_g for each tile of values g to map the original values into the representable dynamic range of FP8:

$$\hat{X}_{\text{FP8}}(X_{i,j}; s_g) = \text{dequantize}(\text{FP8_convert}(X_{i,j} \cdot s_g)) / s_g. \quad (1)$$

To enhance approximation accuracy, tile-wise FP8 quantization employs per-tile scaling factors $\{s_g\}$ that minimize quantization error within each specific tile. This approach preserves attention head-specific and frame-specific activation dynamics while typically reducing data size by half (e.g., from 16-bit to 8-bit). The result is a theoretical $2\times$ reduction in memory bandwidth requirements, with further effective improvements achievable through specialized FP8 hardware acceleration.

Sliding Tile Attention (STA). Standard attention operations on $N = L$ tokens with feature dimension d incur a computational complexity of $\mathcal{O}(N^2d)$, creating a significant bottleneck for high-resolution video generation.

STA addresses this challenge by partitioning the 3D token space into M non-overlapping tiles $\{\mathcal{T}_u\}$ of dimensions (T_t, T_h, T_w) .

The key innovation of STA is its locality-based attention mechanism: each query tile u attends exclusively to key tiles v within a local neighborhood $\mathcal{W}(u)$, defined by the distance constraint:

$$\mathcal{W}(u) = \left\{ v : \|c_u - c_v\|_\infty \leq \left(\frac{W_t}{2T_t}, \frac{W_h}{2T_h}, \frac{W_w}{2T_w} \right) \right\}, \quad (2)$$

where (W_t, W_h, W_w) denote the window dimensions measured in tile units, and c_u, c_v are the centers of tiles u and v . This constraint effectively replaces full attention with a tile-wise masked attention:

$$P_{q,k} = \begin{cases} \text{Softmax}(Q_q K_k^\top / \sqrt{d}), & \text{if token } k \text{ is in a tile } \mathcal{T}_v \text{ where } v \in \mathcal{W}(u), \\ -\infty, & \text{otherwise.} \end{cases} \quad (3)$$

where Q and K are queries and keys. STA generates $M \times |\mathcal{W}(u)|$ dense attention blocks that are compatible with optimized implementations such as FlashAttention[6]. This design provides substantial speedup by replacing the irregular sparse patterns of token-wise sliding window attention with structured tile-based computations that align well with GPU memory hierarchies. As demonstrated in [54], this approach can accelerate attention by 2.8–17 \times over FlashAttention-2[5] and 1.6–10 \times over FlashAttention-3[31] for video generation tasks.

3.2 Joint Tile-wise FP8 Sparse Attention

Building upon FP8 quantization and tiled attention techniques, we introduce **FPSAttention**, a *Joint Tile-wise FP8 Quantization and Sparse Attention* mechanism that synergistically optimizes computational efficiency and accuracy in video DiTs.

Our tile-wise granularity approach (Figure 4, last row) is motivated by three primary considerations. First, it offers an optimal accuracy-efficiency trade-off compared to conventional methods (per-token, per-channel, per-group; Figure 4, first three rows) that often fail to align with underlying hardware architectures. While per-group quantization provides a reasonable balance, it frequently overlooks GPU compute tile patterns, thereby reducing hardware utilization efficiency. Second, our approach maintains full compatibility with the STA sparsity design, allowing seamless integration of quantization and sparsity optimizations at matching granularity. Third, our tile-wise design exhibits superior hardware compatibility, aligning precisely with compute tiles in optimized kernels such as FlashAttention, which enables direct translation of theoretical computational savings into practical speedups.

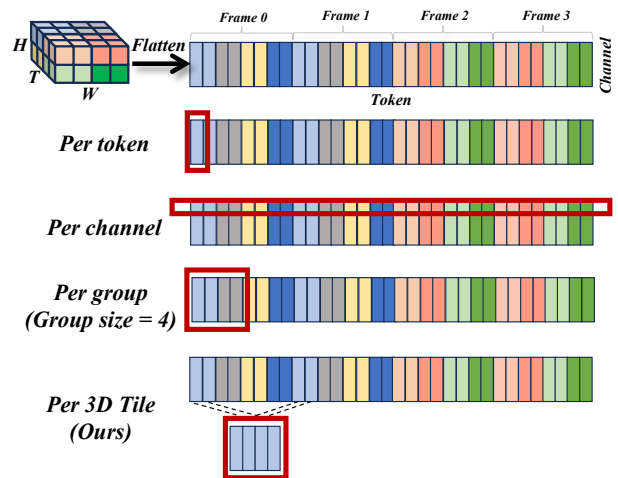


Figure 4 Quantization granularities: per-token, per-channel, per-group, and our per 3D-tile, which aligns with hardware compute patterns.

The **FPSAttention** mechanism processes neural activations through a systematic workflow: (1) organizing query (Q) and key (K) activations into contiguous 3D tiles aligned with GPU cache layouts for enhanced data locality; (2) quantizing each tile to FP8 precision with a locally optimized scale factor; (3) enforcing tile-granularity sparse attention patterns, leveraging spatial locality and low-bit arithmetic; and (4) dequantizing the aggregated attention output to higher precision (BF16/FP16).

Tile-wise FP8 quantization for Q and K . The matrices $Q, K \in \mathbb{R}^{L \times d}$ are partitioned along the sequence dimension L into non-overlapping tiles $\{\mathcal{T}_u\}$ of dimensions (T_t, T_h, T_w) . For each tile \mathcal{T}_u , we compute separate scaling factors s_u^Q and s_u^K to map their values optimally to the FP8 representable range via

$$s_u^Q = \max_{(i,j) \in \mathcal{T}_u} |Q_{i,j}| / M_{\text{FP8_max}}, \quad s_u^K = \max_{(i,j) \in \mathcal{T}_u} |K_{i,j}| / M_{\text{FP8_max}}, \quad (4)$$

where $M_{\text{FP8_max}}$ is the maximum representable magnitude in FP8 and bounded by specific format. Then each element is independently quantized:

$$\hat{Q}_{i,j} = \text{FP8}(Q_{i,j}; s_u^Q), \quad \hat{K}_{i,j} = \text{FP8}(K_{i,j}; s_u^K). \quad (5)$$

This per-tile scaling strategy minimizes quantization error for both Q and K independently, preserving attention dynamics more effectively than global scaling approaches. When combined with the STA formulation, the attention weights P are computed using the quantized \hat{Q} and \hat{K} , following Eq. 3. This formulation enforces a regular, block-sparse pattern (Figure 3) that efficiently maps to modern GPU compute architectures.

Channel-wise FP8 quantization of V and tensor-wise FP8 quantization of P . For the value matrix $V \in \mathbb{R}^{L \times d}$, a channel-wise FP8 quantization is employed. For each channel, we compute the scaling factor s_j^V to map the values optimally to the FP8 representable range: $s_j^V = \max_{i \in L} |V_{i,j}| / M_{\text{FP8_max}}$. Each element in V_j is subsequently quantized as $\hat{V}_j = \text{FP8}(V_j; s_j^V)$. We observe that keeping the fine granularity for V is critical for the performance. Following SageAttention2 [51], we use a fixed scalar $\frac{1}{448}$ to quantize P , obtaining \hat{P} in FP8.

Aggregation and dequantization. The attention output is computed as $\hat{X} = \hat{P}\hat{V}$. This low-precision output is then dequantized to higher precision (BF16/FP16) to maintain computational stability in subsequent layers.

By quantizing Q and K tiles independently while using channel-wise quantization for V , the `FPSAttention` mechanism captures fine-grained statistical properties of each attention component while maintaining optimal alignment with GPU memory hierarchies. Furthermore, the tile-constrained sparse attention pattern creates $M \times |\mathcal{W}(u)|$ dense, structured attention blocks that avoid the inefficiencies of unstructured sparsity patterns. This approach enables direct wall-clock speedups during execution by maximizing hardware utilization and minimizing memory access overhead, as demonstrated in our experimental results.

3.3 Denoising Step-aware Quantization and Sparsity Strategy

The mechanism described in Section 3.2 employs uniform quantization and sparsity across denoising steps. However, as illustrated in Fig. 5, video DiTs exhibit varying sensitivity to numerical precision and sparsity levels throughout the diffusion process. Specifically, early and late denoising steps demonstrate greater tolerance to coarser quantization and higher sparsity, whereas intermediate steps demand finer numerical precision and lower sparsity. This also suggests that diffusion models can intrinsically correct the approximation errors of attention, which motivates our training-aware scheme to mitigate the training-inference gap. Based on these observations, we propose an adaptive, denoising step-aware compression schedule, for both training and inference. We adjust the quantization granularity $g(t)$ and sparsity window size $W(t)$ based on the denoising step t .

Piecewise schedule for quantization and sparsity. For D denoising steps, we partition the process into three regimes using thresholds $t_1 = \alpha_1 D$ and $t_2 = \alpha_2 D$ ($0 < \alpha_1 < \alpha_2 < 1$), each associated with different quantization tile sizes $g(t)$ and sparsity window sizes $W(t)$. Smaller $g(t)$ corresponds to a finer quantization granularity, while larger $W(t)$ indicates a denser attention pattern.

We show quantization and sparsity schedule as following. We define a time-dependent hyperparameter vector $S(t) = [g(t), W(t)]$, which is governed by:

$$S(t) = \begin{cases} [g_{\text{coarse}}, W_{\text{sparse}}], & t \leq t_1 \text{ (Early-Denoising Steps)}, \\ [g_{\text{fine}}, W_{\text{dense}}], & t_1 < t \leq t_2 \text{ (Mid-Denoising Steps)}, \\ [g_{\text{intermediate}}, W_{\text{medium_density}}], & t > t_2 \text{ (Late-Denoising Steps)}, \end{cases} \quad (6)$$

with $g_{\text{coarse}} > g_{\text{intermediate}} > g_{\text{fine}}$ and $W_{\text{dense}} > W_{\text{medium_density}} > W_{\text{sparse}}$, ensuring the finest quantization granularity and densest attention patterns during these mid-denoising steps, as illustrated in Figure 5.

These hyperparameters are selected at inference time to match the model’s varying tolerance to quantization and sparsity across different denoising stages, and then transferred to the training to avoid the prohibitive computational overhead. During training, this configuration allows the model to adaptively compensate for joint quantization-sparsity errors, leading to satisfiable stability and convergence throughout the training process, as shown in Figure 7.

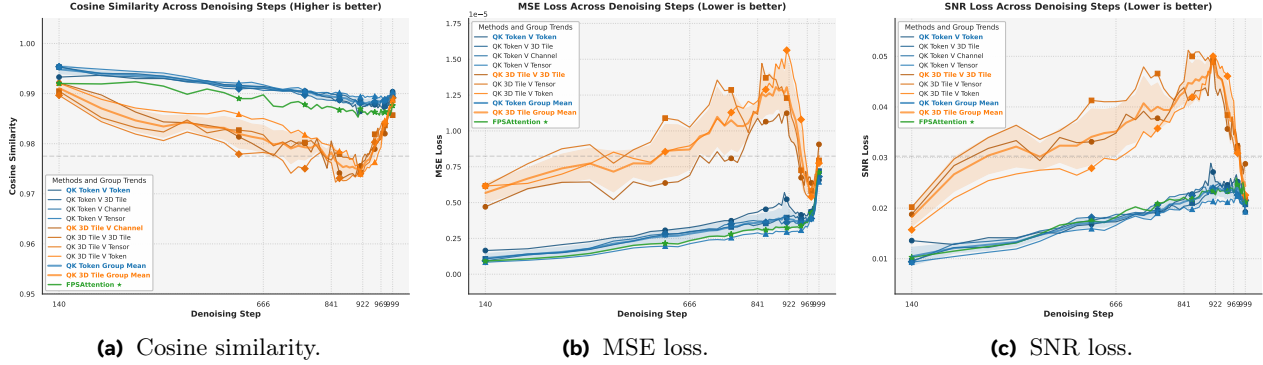


Figure 5 Joint quantization and sparsity error patterns across denoising steps. **Blue**: token-level granularity; **orange**: our 3D tile-wise granularity with sparse attention. Key insight: early/late steps tolerate coarser quantization and higher sparsity, while intermediate steps require finer granularity and denser attention. Our **FPSAttention** (green) closely approximates highest-granularity methods, validating our adaptive scheduling strategy. All measurements from inference are with identical prompts. Performance gaps primarily stem from FP8 quantization rather than sparsity constraints.

3.4 Hardware-Optimized Kernel Design

Our algorithmic designs are complemented by a hardware-optimized kernel implementation for maximum practical efficiency. The implementation addresses several key aspects: memory access coalescing through structured operations that enable efficient GPU memory loads/stores with tiling support; maximized parallelism via tile-wise operations that process independent tiles concurrently; exploitation of dedicated acceleration units such as Tensor Cores on NVIDIA Hopper/Ada architectures for mixed-precision and FP8 computations; and operation fusion that combines multiple logical steps (attention, sparsity, dequantization) into single triton kernels, significantly reducing overhead and memory traffic while maintaining high tensor core utilization and computational intensity.

4 Experiments

Implementation details. We implemented our proposed framework on the Wan2.1[38] architecture (1.3B and 14B variants), preserving the original model structure while introducing **FPSAttention**, joint FP8 quantization and structured sparsity. The quantization schemes and sparsity patterns were applied across attention mechanisms using score mod and mask mod functions via FlexAttention [9]. Fused kernels were compiled using Triton to accelerate inference on Hopper GPUs. The models were trained on high-quality video data (480p×16fps×5s). We trained **FPSAttention** on Wan2.1-14B using 64 nodes with 8 H20 GPUs for 7 days. For detailed hardware specifications, training procedures, dataset preparation, evaluation protocols, and baseline comparisons, please refer to Appendix.

Evaluation protocol. We evaluate our method on the public video dataset, VBench [18]. We following the common practice [57, 20] to sample 5 videos per evaluation prompts defined in the VBench dataset, and assess the video generation quality across 16 VBench dimensions. We also report Peak Signal-to-Noise Ratio (PSNR) [13], Structural Similarity Index (SSIM)[43], and Learned Perceptual Image Patch Similarity (LPIPS) [55] metrics.

4.1 Main Results

Quality evaluation. We compare **FPSAttention** with several state-of-the-art optimization methods, as shown in Table 2. Our baselines include sparsity-based approaches (SparseVideoGen [45] and STA), quantization methods (SageAttention [52]), and hybrid approaches (SpargeAtten [53], a training-free method that jointly applies attention sparsification and activation quantization). As demonstrated in Table 2, **FPSAttention** achieves superior performance across all quality metrics. Particularly notable is the average PSNR of 25.74353 on the Wan2.1-14B model, significantly outperforming all baseline methods. This objective metric

Table 2 Quality and efficiency benchmarking results. [†] We reproduce the results of the baseline methods from the original papers. Note that VBench results here may differ from official results due to the randomness in generated samples and prompt extensions. The quality and efficiency evaluation is based on 480p videos. Specifically, [‡] indicates the speedups via 720p with longer sequence length.

Method	Quality					Efficiency			
	PSNR \uparrow	SSIM \uparrow	LPIPS \downarrow	ImageQual \uparrow	SubConsist \uparrow	FLOPS \downarrow	Latency \downarrow	Speedup \uparrow	Speedup [‡] \uparrow
Wan2.1-1.3B [†]	-	-	-	0.6708	0.9536	77.52 PFLOPS	271s	1.00x	-
SageAttention	20.18990	0.78241	0.18811	0.6699	0.9453	37.61 PFLOPS	141s	1.91x	-
SpargAtten	17.72979	0.72628	0.26183	0.6541	0.8982	43.15 PFLOPS	205s	1.32x	-
SparseVideoGen	19.51276	0.78891	0.20513	0.6729	0.9292	30.67 PFLOPS	152s	1.78x	-
STA	18.78546	0.76335	0.23187	0.6626	0.8992	31.78 PFLOPS	143s	1.89x	-
Ours Quant	20.99712	0.79820	0.15114	0.6798	0.9458	32.01 PFLOPS	144s	1.88x	-
Ours Quant + Sparse	21.35417	0.80835	0.15398	0.7103	0.9338	32.01 PFLOPS	110s	2.45x	-
Wan2.1-14B [†]	-	-	-	0.6715	0.9528	637.52 PFLOPS	1301s	1.00x	1.00x
SageAttention	24.33985	0.82283	0.15607	0.6724	0.9530	301.98 PFLOPS	646s	2.01x	1.94x
SpargAtten	21.38291	0.81452	0.21723	0.6350	0.9173	339.30 PFLOPS	734s	1.77x	2.12x
SparseVideoGen	23.52881	0.80113	0.17032	0.6868	0.9489	259.79 PFLOPS	613s	2.12x	3.13x
STA	22.65635	0.82024	0.19283	0.6577	0.9530	264.34 PFLOPS	548s	2.37x	3.60x
Ours Quant + Sparse	25.74353	0.83171	0.07610	0.7103	0.9435	273.01 PFLOPS	423s	3.07x	4.96x

Baseline, Wan2.1 1.3B, 1 \times E2E speedup

Our FPSAttention, 4.96 \times E2E speedup

Figure 6 Examples of generated videos by FPSAttention and the Wan2.1 1.3B baseline. We showcase from five different aspects. FPSAttention achieves 4.96 \times E2E speedup, while maintaining lossless visual quality. Please click the image to play the video clip via Acrobat Reader.

confirms FPSAttention’s ability to generate videos with exceptional fidelity to reference images. Furthermore, FPSAttention maintains excellent performance on perceptual metrics, with high Video Quality (0.7103) and strong spatial-temporal consistency (0.9435) on the VBench evaluation. Interestingly, after joint training, FPSAttention exhibits a slight increase in VBench scores, while [50, 54] also demonstrate performance improvements when trained with structured sparsity—potentially driven by the inductive bias of locality. These results validate that our joint sparsity and quantization approach preserves visual quality while substantially improving computational efficiency. Visual examples in Figure 6 further illustrate that FPSAttention **consistently outperforms** baseline methods while maintaining quality comparable to the original model.

Test-time efficiency. We evaluate computational efficiency across both 1.3B and 14B parameter variants of the Wan2.1 model, as reported in Table 2. For the 1.3B parameter model, FPSAttention achieves up to 2.45 \times speedup on 480p videos while maintaining superior quality metrics. More impressively, when tested on the larger 14B parameter model with 720p videos (indicated by [‡] in the table), FPSAttention achieves a substantial **4.96 \times end-to-end speedups** compared to the baseline.

4.2 Ablation Study

In this section, we conduct a comprehensive ablation study to analyze the effects of key components in **FPSAttention**. We investigate the different tile size selection for quantization and sparsity, and the relations to the hardware awareness. Additionally, we investigate how sparsity window dimensions affect model performance and computational efficiency. We also study the training stability to verify whether our **FPSAttention** training dynamics highly aligns the baseline trend.

Effect of tile size for quantization and sparsity. We investigate the impact of joint quantization and sparsity granularity by varying tile sizes along temporal (t), height (h), and width (w) dimensions, with results presented in Table 3. Our experiments demonstrate that the largest tile configuration (24,32,32) achieves optimal performance with PSNR 20.99712, SSIM 0.79820, and LPIPS 0.15114. However, we observe minimal performance differences between configurations (6,8,8), (12,16,16), and (24,32,32). Based on these findings, we implement a scheduled approach, using different tile sizes for early, mid, and late denoising steps, respectively. We emphasize the hardware-friendly configuration of (6,8,8) yields the best throughput as it aligns with flash attention block size design and is optimized for the Hopper architecture. Notably, unbalanced tile sizes, such as (3,4,4), lead to significant performance degradation, this configuration is also misalign with flash attention block size leads to inefficiency.

Effect of sparsity window dimensions. The relationship between sparsity window dimensions, inference speed, and model performance is analyzed in Table 4. Our results demonstrate that a configuration (6,6,1) using temporal window of 6, height window of 6, and width window of 1 provides an optimal balance, achieving a substantial 5.16 \times kernel speed-up while maintaining high visual quality. This suggests that while reducing the temporal and spatial window sizes improves efficiency, there exists a threshold beyond which visual quality deteriorates significantly.

Training stability. Joint FP8 quantization and structured sparsity initially increases training loss by 15% compared to full-precision Wan2.1 baseline (Figure 7). We mitigate these challenges through adaptive learning rate scheduling and gradient accumulation techniques. After 2,000 steps, loss convergence trajectories become nearly identical (<2% difference), confirming that our FP8 sparse attention preserves critical information pathways despite bitwidth and sparsity constraints.

5 Conclusion and Future Work

In this paper, we have introduced **FPSAttention**, a module jointly optimizing FP8 quantization and structured sparsity for video diffusion models. Through unified 3D tile-wise granularity, denoising step-aware adaptation, and hardware-friendly kernel implementation, our approach achieves up to 7.09 \times kernel speedup and 4.96 \times end-to-end acceleration without compromising generation quality. The tile-aligned approach ensures quantization and sparsity work synergistically, while step-aware scheduling adapts compression hyperparameters to varying sensitivity across diffusion phases. Despite these results, our approach has limitations: it performs best on FP8-supporting hardware, requires additional training resources, and introduces certain hyperparameters. We currently validate **FPSAttention** on Wan2.1 due to resource constraints. Future work will focus on broadening the applicability by generalizing beyond specific architectures (e.g. Hunyuan [18] based on MMDiT [10]).

Table 3 Effect of different tile sizes on model performance on Wan2.1 1.3B. We evaluate various tile size combinations for temporal (t), height (h), and width (w) dimensions.

Tile Size			Metrics		
t	h	w	PSNR \uparrow	SSIM \uparrow	LPIPS \downarrow
3	4	4	19.87452	0.77634	0.16521
6	8	8	20.12358	0.78147	0.15982
12	16	16	20.45621	0.78932	0.15743
24	32	32	20.99712	0.79820	0.15114

Table 4 Impact of sparsity window dimensions on model performance and computational efficiency. We evaluate various combinations of temporal (t), height (h), and width (w) window sizes and measure inference kernel speedup.

Window Size			Metrics			
t	h	w	PSNR \uparrow	SSIM \uparrow	LPIPS \downarrow	Speedup \uparrow
3	3	1	19.23465	0.76128	0.17251	3.24x
5	6	10	19.94731	0.77926	0.16327	3.07x
6	6	6	20.12482	0.78341	0.16014	1.69x
6	6	1	20.45621	0.78932	0.15743	5.16x

Training Loss Comparison

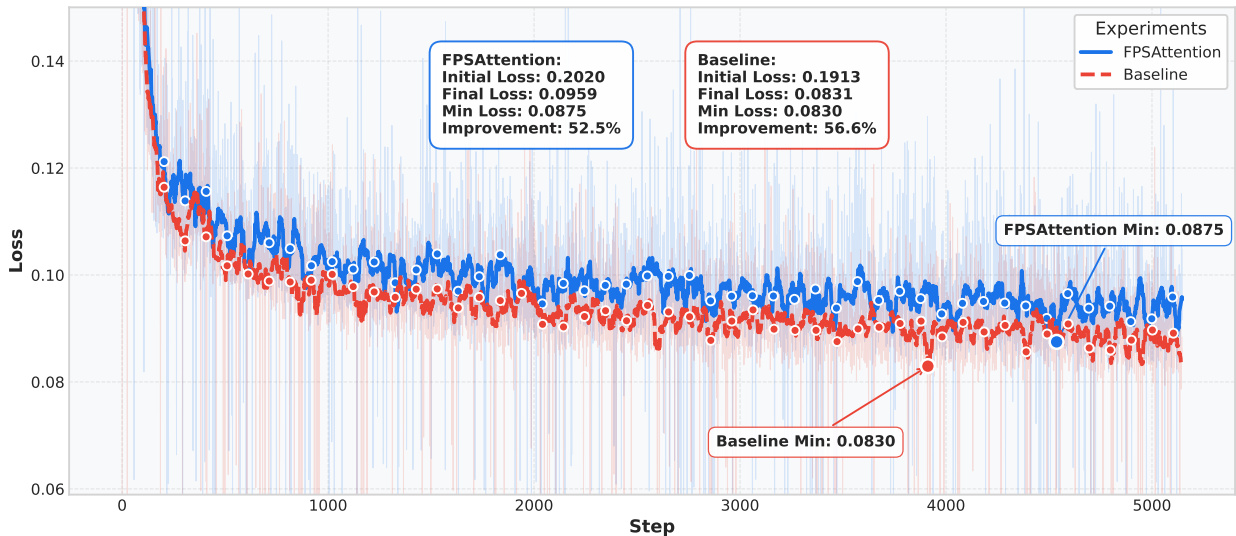


Figure 7 Training loss comparison between baseline Wan2.1 1.3B, and our joint FP8 quantization with structured sparsity. The FPSAttention shows slightly higher loss initially but stabilizes with comparable final performance.

We also aim to refine training resource requirements and hyperparameter management, and extend these co-design principles beyond attention mechanisms to other model components. Furthermore, FPSAttention is orthogonal to step distillation techniques [30, 49]. By incorporating step distillation, additional acceleration can be achieved.

6 Contributions

This work represents a collaborative effort across multiple institutions and researchers. The following details the specific contributions and affiliations of each author:

Author Contributions:

- **Co-first authors (*):** Akide Liu and Zeyu Zhang contributed equally to this work, with primary responsibility for method design, theoretical analysis, and experimental validation.
- **Co-second authors (†):** Zhixin Li and Xuehai Bai contributed equally as co-second authors, focusing on implementation details, algorithm optimization, and evaluation framework development.
- **Project leads (‡):** Jiasheng Tang and Bohan Zhuang served as the project leads, providing overall direction, coordination, and strategic guidance throughout the research.

Internship Affiliations:

- **Intern at DAMO Academy:** Akide Liu and Zeyu Zhang conducted their research as interns at DAMO Academy, Alibaba Group.
- **Intern at Zhejiang University:** Xuehai Bai conducted research as an intern at Zhejiang University.

All authors contributed to the writing and revision of the manuscript. The experimental work was conducted collaboratively across all participating institutions, with computational resources primarily provided by DAMO Academy’s infrastructure.

Acknowledgement: This work was supported by Damo Academy (Hupan Laboratory) through Damo Academy (Hupan Laboratory) Research Fellow Program.

Appendix

Contents

A	FPSAttention Algorithm	12
B	Additional Implementation Details	13
C	Ablation Study: Challenges of Naive Quantization and Sparsity Combination	13
D	VBench Full Evaluation Results	15
E	Clarification on VBench Evaluation Metrics	15
F	Training Hyperparameters	16
G	Limitations	17
H	Visualization	18

A FPSAttention Algorithm

Algorithm 1 presents the core computational workflow of our FPSAttention method, which implements joint tile-wise FP8 quantization with structured sparse attention and denoising step-aware adaptation. The algorithm follows the methodology described in the main paper, incorporating tile-wise quantization for queries and keys, channel-wise quantization for values, tensor-wise quantization for attention weights, and dynamic adaptation based on denoising timesteps.

Algorithm 1 FPSAttention: Joint Tile-wise FP8 Quantization and Sparse Attention

Input: Input tensors $Q, K, V \in \mathbb{R}^{L \times d}$, denoising step t , diffusion steps D
Input: Transition points α_1, α_2 , quantization granularities $\{g_{\text{coarse}}, g_{\text{fine}}, g_{\text{intermediate}}\}$
Input: Window sizes $\{W_{\text{sparse}}, W_{\text{dense}}, W_{\text{medium_density}}\}$, tile scheme \mathcal{T}
Output: Output tensor $X \in \mathbb{R}^{L \times d}$ (BF16/FP16)

```

1: // 1. Denoising Step-aware Parameter Selection
2:  $t_1 \leftarrow \alpha_1 \cdot D, t_2 \leftarrow \alpha_2 \cdot D$ 
3: if  $t \leq t_1$  then
4:    $g(t) \leftarrow g_{\text{coarse}}, W(t) \leftarrow W_{\text{sparse}}$  // Early steps
5: else if  $t_1 < t \leq t_2$  then
6:    $g(t) \leftarrow g_{\text{fine}}, W(t) \leftarrow W_{\text{dense}}$  // Mid steps
7: else
8:    $g(t) \leftarrow g_{\text{intermediate}}, W(t) \leftarrow W_{\text{medium\_density}}$  // Late steps
9: end if
10: // 2. Tile-wise FP8 Quantization for Q and K
11: Partition  $Q, K$  into tiles  $\{\mathcal{T}_u\}$  with granularity  $g(t)$ 
12: for each tile  $\mathcal{T}_u$  do
13:    $s_u^Q \leftarrow \max_{(i,j) \in \mathcal{T}_u} |Q_{i,j}| / M_{\text{FP8\_max}}$ 
14:    $s_u^K \leftarrow \max_{(i,j) \in \mathcal{T}_u} |K_{i,j}| / M_{\text{FP8\_max}}$ 
15:    $\hat{Q}_{i,j} \leftarrow \text{FP8}(Q_{i,j}; s_u^Q)$  for  $(i, j) \in \mathcal{T}_u$ 
16:    $\hat{K}_{i,j} \leftarrow \text{FP8}(K_{i,j}; s_u^K)$  for  $(i, j) \in \mathcal{T}_u$ 
17: end for
18: // 3. Channel-wise FP8 Quantization for V
19: for each channel  $j \in \{1, \dots, d\}$  do
20:    $s_j^V \leftarrow \max_{i \in L} |V_{i,j}| / M_{\text{FP8\_max}}$ 
21:    $\hat{V}_{i,j} \leftarrow \text{FP8}(V_{i,j}; s_j^V)$  for all  $i$ 
22: end for
23: // 4. Structured Sparse Attention Computation via FlexAttention
24: Define neighborhood  $\mathcal{W}(u)$  based on window size  $W(t)$ :
25:  $\mathcal{W}(u) = \{v : \|c_u - c_v\|_\infty \leq (W_t/(2T_t), W_h/(2T_h), W_w/(2T_w))\}$ 
26: // Configure FlexAttention mask and score modification functions
27: Define  $\text{mask\_mod}(b, h, q, k) = \text{True}$  if  $\text{tile}(q) \in \mathcal{W}(\text{tile}(k))$ , False otherwise
28: Define  $\text{score\_mod}(S, b, h, q, k) = S$  // Identity for quantized inputs
29: // Execute FlexAttention with quantized inputs and custom modifications
30:  $\hat{X} \leftarrow \text{FlexAttention}(\hat{Q}, \hat{K}, \hat{V}, \text{score\_mod}, \text{mask\_mod})$ 
31: // 5. Dequantize Output to Target Precision
32:  $X \leftarrow \text{Dequantize}(\hat{X})$  // Dequantize to BF16/FP16
return  $X$ 

```

Key Algorithmic Components

The algorithm implements the four core innovations described in the main paper:

- **Denoising Step-aware Adaptation:** Lines 2-8 implement the adaptive scheduling strategy from Equation 6 in the main paper, dynamically adjusting quantization granularity $g(t)$ and sparsity window size $W(t)$ based on the current denoising step t .

- **Tile-wise FP8 Quantization for Q and K:** Lines 10-15 partition queries and keys into 3D tiles with step-dependent granularity and compute per-tile scaling factors s_u^Q and s_u^K to minimize quantization error within each tile.
- **Channel-wise FP8 Quantization for V:** Lines 17-20 apply channel-wise quantization to the value matrix, preserving fine-grained channel information that is critical for generation quality.
- **FlexAttention-based Sparse Attention:** Lines 22-26 implement structured sparse attention using FlexAttention’s `mask_mod` and `score_mod` interfaces, enabling hardware-optimized execution with tile-wise sparsity patterns that generate exactly $M \times |\mathcal{W}(u)|$ dense attention blocks.
- **Output Dequantization:** Line 28 dequantizes the FlexAttention output to the target precision (BF16/FP16) to maintain compatibility with the downstream network components.

This implementation ensures full compatibility with the theoretical framework while enabling practical hardware acceleration through structured computation patterns and optimal memory access patterns.

B Additional Implementation Details

Models. We implement and evaluate FPSAttention on the Wan architecture [39], leveraging both 1.3B and 13B parameter variants to demonstrate scalability. The Wan models feature a DiT backbone with cross-attention for text conditioning and temporal attention for inter-frame modeling. Our implementation maintains architectural fidelity while seamlessly integrating FP8 quantization across attention and feed-forward components. The joint quantization and sparsity mechanisms are realized through FlexAttention’s score and mask modification interfaces, with the resulting fused kernels compiled via Triton for optimal execution on Hopper architectures.

Hardware. Experiments utilize a distributed computing cluster with high-performance GPU nodes, each containing 192 CPU cores, 960GB system memory, and $8 \times$ NVIDIA H20 GPUs (96GB each). InfiniBand interconnects ensure high-bandwidth inter-node communication for distributed training. Training scales from 16 nodes (1.3B model) to 64 nodes (13B model), requiring approximately 7 days per configuration to achieve convergence.

Dataset. Training employs a curated high-quality video dataset processed through a comprehensive filtering pipeline. The preprocessing workflow includes automated subtitle removal, black-border cropping, and monochrome video exclusion, followed by quality-based filtering using established metrics (Q-Align > 3.5 , Aesthetic Score > 2.0 , optical flow magnitude 0.05–2.0). After deduplication, videos are standardized to 480p resolution, 16fps frame rate, and 5-second duration to optimize the computational efficiency-quality balance across both model scales.

Evaluation. Performance assessment utilizes the VBench benchmark [18], following established protocols [57, 20] with 5-video sampling per prompt. Evaluation encompasses 16 comprehensive VBench dimensions covering aesthetic quality, temporal consistency, motion dynamics, and semantic understanding. Additional quantitative metrics include PSNR [13], SSIM, and LPIPS [55] to provide multi-faceted quality assessment.

Baselines. Our comparative analysis includes representative approaches from three categories: (1) sparsity-based methods (SparseVideoGen [45], STA), (2) quantization-focused techniques (SageAttention [52]), and (3) joint optimization methods (SpargeAttn [53]). This selection enables comprehensive evaluation of FPSAttention against both specialized single-optimization approaches and competing joint methods, providing a thorough assessment of our framework’s relative performance and efficiency gains.

C Ablation Study: Challenges of Naive Quantization and Sparsity Combination

To validate our core motivation that naive combination of FP8 quantization and sparsity presents significant challenges, we conduct a comprehensive ablation study comparing three key approaches: (1) the baseline full-precision model, (2) a training-free naive combination of quantization and sparsity, and (3) our proposed FPSAttention method with joint optimization.

Table 5 presents a detailed comparison across all VBench metrics for the Wan 1.3B model. The training-free approach applies standard FP8 quantization and sparse attention patterns without joint optimization or denoising step-aware adaptation. As hypothesized, this naive combination leads to substantial performance degradation across nearly all evaluation metrics.

Table 5 Ablation study demonstrating the challenges of naive quantization and sparsity combination. We compare baseline full-precision (Baseline), training-free naive combination (Training-Free), and our joint optimization approach (FPSAttention) on Wan 1.3B across all VBench metrics. The severe degradation in the training-free approach validates the need for holistic joint optimization.

Metric	Baseline	Training-Free	FPSAttention
Aesthetic Quality	0.6105	0.2892	0.6240
Appearance Style	0.7157	0.7874	0.7252
Background Consistency	0.9503	0.9280	0.9156
Color	0.9049	0.4836	0.8932
Dynamic Degree	0.3014	0.3750	0.4195
Human Action	0.7720	0.0200	0.7780
Imaging Quality	0.6708	0.6868	0.7103
Motion Smoothness	0.9527	0.9513	0.9413
Multiple Objects	0.6091	0.0000	0.6665
Object Class	0.7710	0.0109	0.8185
Overall Consistency	0.6453	0.1206	0.6893
Quality Score	0.8332	0.7473	0.8428
Scene	0.3030	0.0129	0.3870
Semantic Score	0.6768	0.1733	0.7088
Spatial Relationship	0.7317	0.0008	0.7659
Subject Consistency	0.9457	0.8887	0.9338
Temporal Flickering	0.9844	0.9401	0.9336
Temporal Style	0.6382	0.1239	0.6558
Total Score	0.8019	0.6325	0.8160
Performance Drop	–	-21.1%	+1.8%

Key Findings: The results clearly demonstrate the challenges inherent in naive quantization and sparsity combination:

- **Severe Quality Degradation:** The training-free approach achieves only 0.6325 total score compared to the baseline’s 0.8019, representing a substantial 21.1% performance drop.
- **Critical Failure Modes:** Several metrics show near-zero performance in the training-free approach, including Human Action (0.02), Multiple Objects (0.0), Object Class (0.011), and Spatial Relationship (0.0008), indicating complete failure in complex semantic understanding tasks.
- **Magnified Quantization Errors:** As predicted by our theoretical analysis, sparsity mechanisms amplify quantization errors in high-magnitude attention scores. This is particularly evident in metrics requiring fine-grained semantic understanding, where the interaction between quantization noise and sparse token selection leads to catastrophic information loss.
- **Joint Optimization Success:** In contrast, our FPSAttention approach not only avoids the degradation seen in naive combination but actually improves upon the baseline (0.8160 vs 0.8019, +1.8% improvement), validating the effectiveness of our denoising step-aware joint optimization strategy.

This ablation study emphasizes the necessity of our training-aware co-design scheme.

D VBench Full Evaluation Results

Tables 6 and 7 present comprehensive evaluation results of our method compared to various baselines on VBench for Wan 1.3B and Wan 13B models, respectively. These results demonstrate the effectiveness of our joint FP8 quantization and sparsity approach across multiple video quality metrics.

Table 6 shows performance comparisons across seven methods on the Wan 1.3B model: the baseline (Base), SageAttention (SageAtt) [52], SpargeAttention (SpargeAtt) [53], SparseVideoGen (SparseVG) [45], Sliding Tile Attention (STA) [54], our quantization-only variant (Ours-Q), and our full joint quantization and sparsity method (Ours-Q+S). The evaluation covers 18 comprehensive metrics including aesthetic quality, motion dynamics, temporal consistency, and semantic understanding. Our full method (Ours-Q+S) achieves the highest total score of 0.8160, demonstrating superior performance compared to methods that apply quantization or sparsity independently.

Table 7 presents similar comparisons for the larger 13B model, where our method continues to achieve competitive performance while providing substantial computational savings. The results validate that our approach scales effectively to larger model sizes while maintaining video generation quality across diverse evaluation criteria.

Table 6 Performance comparison of different methods on Wan 1.3B across VBench metrics. We compare the baseline (Base), SageAttention (SageAtt), SpargeAttention (SpargeAtt), SparseVideoGen (SparseVG), Sliding Tile Attention (STA), our quantization-only variant (Ours-Q), and our full joint method (Ours-Q+S). Bold values indicate the best performance for each metric.

Metric	Base	SageAtt	SpargeAtt	SparseVG	STA	Ours-Q	Ours-Q+S
Aesthetic Quality	0.6105	0.6104	0.5668	0.563	0.5661	0.6091	0.624
Appearance Style	0.7157	0.715	0.7744	0.2253	0.7952	0.6922	0.7252
Background Consistency	0.9503	0.95	0.9123	0.9525	0.9284	0.9472	0.9156
Color	0.9049	0.8866	0.8903	0.9037	0.8974	0.9146	0.8932
Dynamic Degree	0.3014	0.307	0.3222	0.7139	0.5722	0.3222	0.4195
Human Action	0.772	0.75	0.734	0.73	0.622	0.75	0.778
Imaging Quality	0.6708	0.6699	0.6541	0.6729	0.6626	0.6798	0.7103
Motion Smoothness	0.9527	0.9527	0.9139	0.9726	0.9649	0.9496	0.9413
Multiple Objects	0.6091	0.5837	0.4715	0.471	0.4043	0.6011	0.6665
Object Class	0.7710	0.7695	0.6859	0.6935	0.5818	0.7851	0.8185
Overall Consistency	0.6453	0.6451	0.6492	0.6935	0.6236	0.6478	0.6893
Quality Score	0.8332	0.8337	0.8049	0.2336	0.7994	0.8363	0.8428
Scene	0.3030	0.3092	0.2192	0.1732	0.1995	0.3200	0.3870
Semantic Score	0.6768	0.6704	0.6412	0.6342	0.6012	0.6780	0.7088
Spatial Relationship	0.7317	0.7364	0.7217	0.6469	0.6863	0.7438	0.7659
Subject Consistency	0.9457	0.9453	0.8982	0.9292	0.8993	0.9458	0.9338
Temporal Flickering	0.9844	0.9841	0.9647	0.9883	0.9652	0.9822	0.9336
Temporal Style	0.6382	0.6385	0.6247	0.2265	0.6005	0.6475	0.6558
Total Score	0.8019	0.8011	0.7722	0.7827	0.7597	0.8046	0.8160

E Clarification on VBench Evaluation Metrics

In this study, we observed that some of the baseline methods we reproduced (including some of our own exploratory experiments prior to FPSAttention) might yield VBench scores slightly lower than those reported in their respective official publications. We attribute this primarily to the following factors: Randomness: The inherent stochasticity in video generation models can lead to slight variations in results and vBench scores across multiple runs, even with identical settings. Prompt Extension: Many prior works [22] may employ specific prompt extension strategies to enrich input prompts. This can influence the content and quality scores of the generated videos. We didn't employ this optimization. Classifier-Free Guidance (CFG) Scale and Other Sampling Strategies: Different CFG scale values and other sampling parameters (e.g., number of sampling steps) significantly impact generation quality. While we endeavored to follow the descriptions in the respective

baseline papers, subtle parameter differences might still exist. It is worth noting that similar observations have been made in other research. For instance, in the work on Sliding Tile Attention (STA) [54], their reproduced HunyuanVideo baseline also exhibited lower VBench performance compared to VBench’s official leaderboard. Despite these potential metric variations, we emphasize that all methods in this study (including our FPSAttention and all compared baselines) were evaluated under an identical VBench evaluation pipeline and parameter settings, ensuring a fair comparison. Our primary research objective is to demonstrate the significant inference speedup achieved by FPSAttention while maintaining comparable (or superior) generation quality relative to baseline methods.

Table 7 Performance comparison of different methods on Wan 13B across VBench metrics. We compare the baseline (Base), SageAttention (SageAtt), SpargeAttention (SpargeAtt), SparseVideoGen (SparseVG), Sliding Tile Attention (STA), and our full joint method (Ours-Q+S). Bold values indicate the best performance for each metric.

Metric	Base	SageAtt	SpargeAtt	SparseVG	STA	Ours-Q+S
Aesthetic Quality	0.6204	0.6209	0.5875	0.6246	0.6033	0.624
Appearance Style	0.2164	0.2163	0.7586	0.2306	0.2303	0.2073
Background Consistency	0.9691	0.9687	0.9355	0.9589	0.9573	0.9377
Color	0.8879	0.8825	0.8768	0.8883	0.8814	0.8932
Dynamic Degree	0.6944	0.7028	0.6028	0.6806	0.7028	0.8389
Human Action	0.796	0.8	0.78	0.816	0.778	0.816
Imaging Quality	0.6715	0.6724	0.635	0.6868	0.6577	0.7103
Motion Smoothness	0.9828	0.9828	0.9413	0.982	0.9714	0.9804
Multiple Objects	0.6627	0.6477	0.6066	0.7012	0.6576	0.666
Object Class	0.8299	0.8312	0.7896	0.8712	0.81	0.8185
Overall Consistency	0.6912	0.6912	0.6975	0.708	0.6893	0.6893
Quality Score	0.6577	0.8428	0.8134	0.7421	0.8246	0.7103
Scene	0.3669	0.3049	0.3495	0.4129	0.3387	0.3182
Semantic Score	0.7572	0.7091	0.6969	0.7421	0.7077	0.7088
Spatial Relationship	0.7364	0.7405	0.7526	0.8056	0.7405	0.7661
Subject Consistency	0.9528	0.953	0.9173	0.9489	0.953	0.9435
Temporal Flickering	0.9922	0.9922	0.969	0.9891	0.9922	0.9754
Temporal Style	0.2408	0.2408	0.6607	0.2438	0.2408	0.6558
Total Score	0.8153	0.8158	0.7901	0.8196	0.8012	0.816

The results demonstrate that our joint FP8 quantization and sparsity approach achieves competitive or superior performance compared to specialized methods focusing solely on either quantization or sparsity. For the Wan 1.3B model, our method achieves the highest total score (0.8160), outperforming the baseline (0.8019) while providing significant computational benefits. Similarly, for the Wan 13B model, our approach performs on par with the best-performing methods while offering substantial memory and compute savings through the combination of quantization and structured sparsity.

F Training Hyperparameters

Table 8 presents the key hyperparameters used in our experiments for both Wan 1.3B and 13B model training configurations. These hyperparameters were carefully selected to balance training stability, convergence speed, and final model performance while accommodating the constraints imposed by FP8 quantization and structured sparsity.

Table 8 Comprehensive hyperparameter configuration for Wan 1.3B and 13B model training and evaluation. The table covers model architecture specifications, training parameters, diffusion scheduler settings, data configuration, and system-level precision settings used in our experiments.

Category	Parameter	Wan 1.3B	Wan 13B
Model Architecture	Model Type	WanX21FPS	WanX21FPS-13B
	Model Dimension	1536	5120
	Number of Layers	30	40
	Number of Heads	12	40
	FFN Dimension	8960	13824
	Input/Output Dimension	16	16
	Frequency Dimension	256	256
	Text Dimension	4096	4096
	Patch Size	[1, 2, 2]	[1, 2, 2]
Training	Learning Rate	5e-6	5e-6
	Weight Decay	1e-4	1e-4
	Gradient Clipping	1.0	1.0
	Warmup Steps	200	200
	EMA Decay	0.99	0.99
	Adam Epsilon	1e-15	1e-15
	Diffusion Scheduler	Scheduler Type	rflow-wanx
Number of Timesteps		1000	1000
Sample Steps		50	50
CFG Scale		5.0	5.0
Sample Shift		5.0	5.0
Transform Scale		5.0	5.0
Sample Method		logit-normal	logit-normal
Data & Sequence	Text Length	512	512
	Max Sequence Length	75600	75600
	Sample FPS	16	16
	Video Resolution	480p	480p
	Video Duration	5s	5s
	Prompt Uncond Probability	0.1	0.1
System & Precision	Data Type	fp8	fp8
	Training Mode	FSDP	FSDP
	Gradient Checkpointing	True	True
	Quantization	True	True
	Sequence Parallel Degree	1	4

G Limitations

While FPSAttention demonstrates strong performance across our evaluation scenarios, there are some considerations for broader adoption. Our approach works best with modern FP8-capable GPUs such as NVIDIA Hopper architectures, though it can still provide benefits on older hardware with reduced FP8 acceleration. The method benefits from quantization-aware training to achieve optimal results, which involves a moderate increase in training time compared to post-training quantization approaches. The denoising step-aware scheduling includes several hyperparameters (transition points α_1 and α_2 , quantization granularities, and window sizes) that can be optimized for different model architectures and datasets. Our current evaluation focuses on the Wan2.1 architecture, and the approach shows strong promise for extension

to other video diffusion transformer architectures (e.g., HunyuanVideo, CogVideoX). Additionally, while our tile-wise approach achieves good hardware utilization across tested configurations, there are opportunities for architecture-specific optimization to further improve performance on different GPU memory hierarchies.

H Visualization

The following qualitative comparison demonstrates that our FPSAttention method generates video frames that are visually nearly identical to the baseline Wan model with size of 1.3B. This visual similarity across diverse scenarios—including boats, fish, dogs, desert landscapes, couples, trains, cars, cats, and robot DJs—validates that our joint FP8 quantization and sparsity optimization achieves essentially lossless performance while providing substantial computational acceleration.

Table 9 Qualitative comparison on the boat group. Prompt: ‘A boat sailing leisurely along the Seine River with the Eiffel Tower in background in super slow motion’. Top: Baseline; Bottom: FPSAttention.

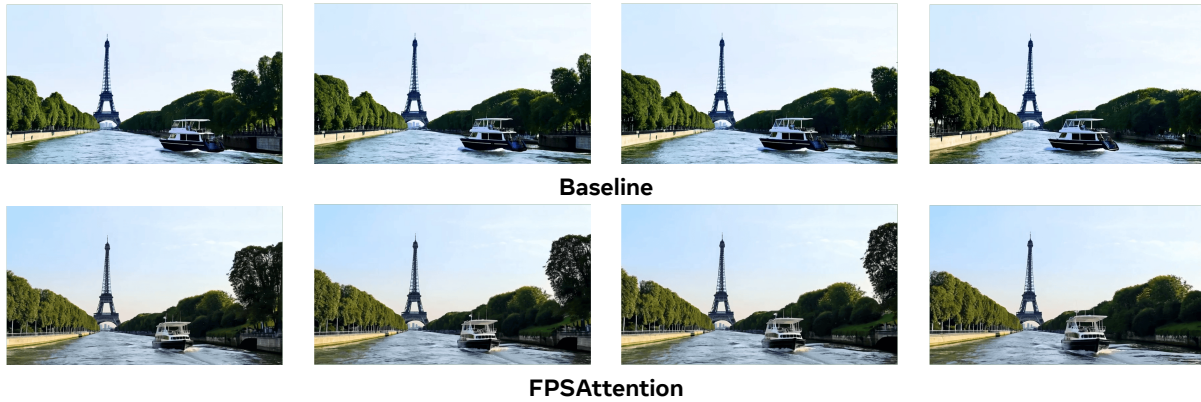


Table 10 Qualitative comparison on the fish group. Prompt : ‘Golden fish swimming in the ocean’. Top: Baseline; Bottom: FPSAttention.

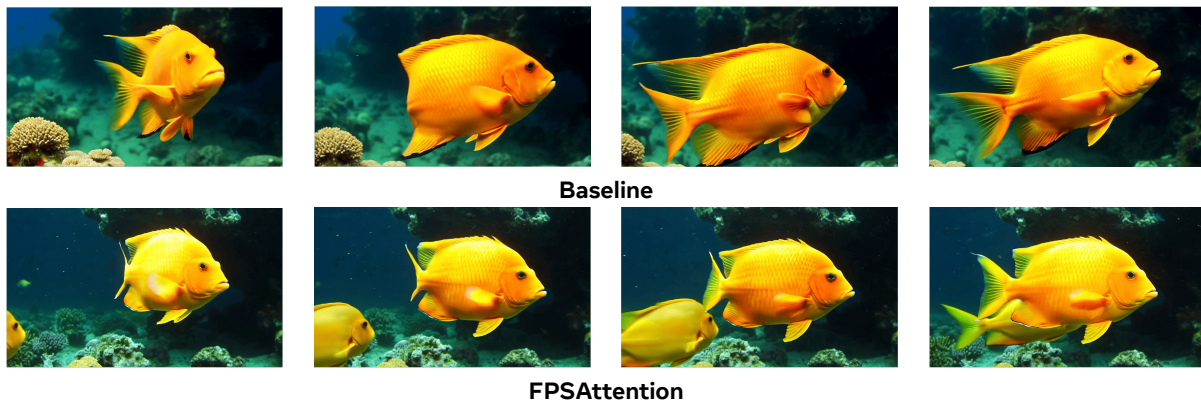


Table 11 Qualitative comparison on the dog group. Prompt: ‘A dog enjoying a peaceful walk’. Top: Baseline; Bottom: FPSAttention.

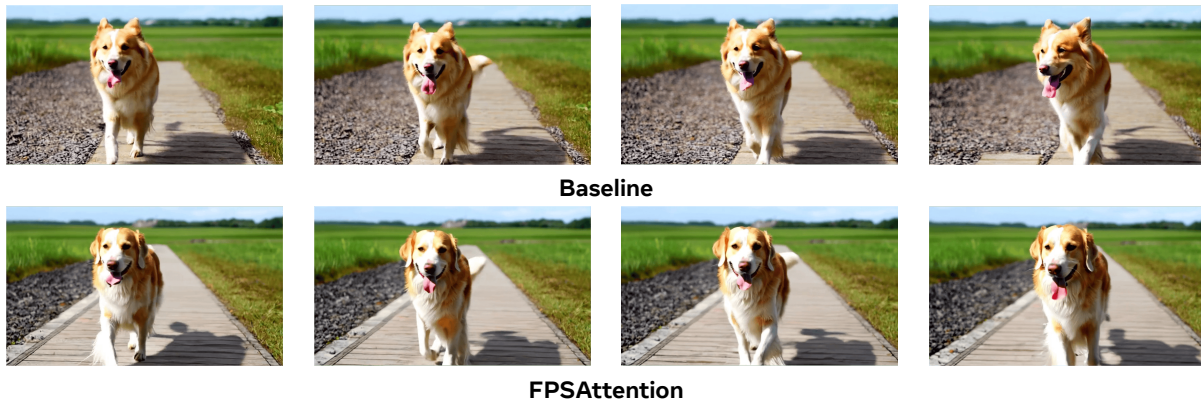


Table 12 Qualitative comparison on the desert group. Prompt: ‘Static view on a desert scene with an oasis palm trees and a clear calm pool of water’. Top: Baseline; Bottom: FPSAttention.

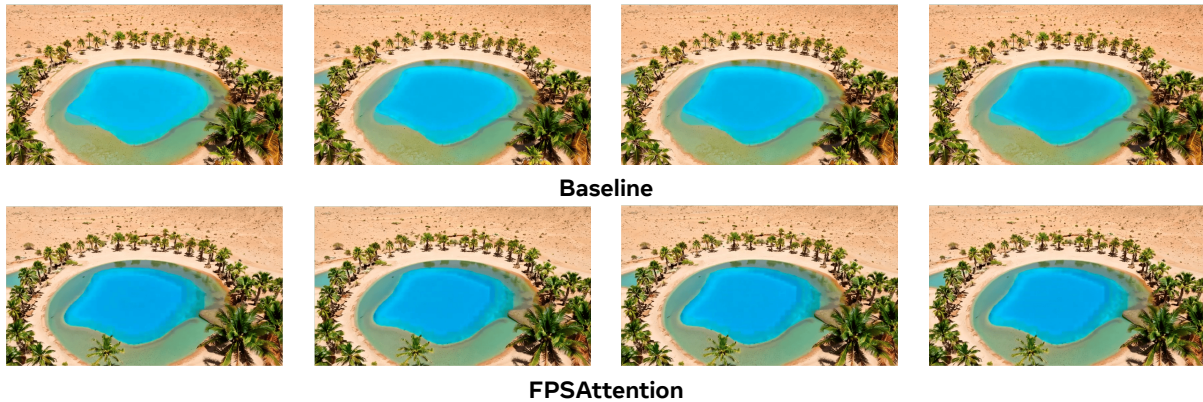


Table 13 Qualitative comparison on the couple group. Prompt: ‘A couple in formal evening wear going home get caught in a heavy downpour with umbrellas’. Top: Baseline; Bottom: FPSAttention.



Table 14 Qualitative comparison on the train group. Prompt: ‘A train accelerating to gain speed’. Top: Baseline; Bottom: FPSAttention.

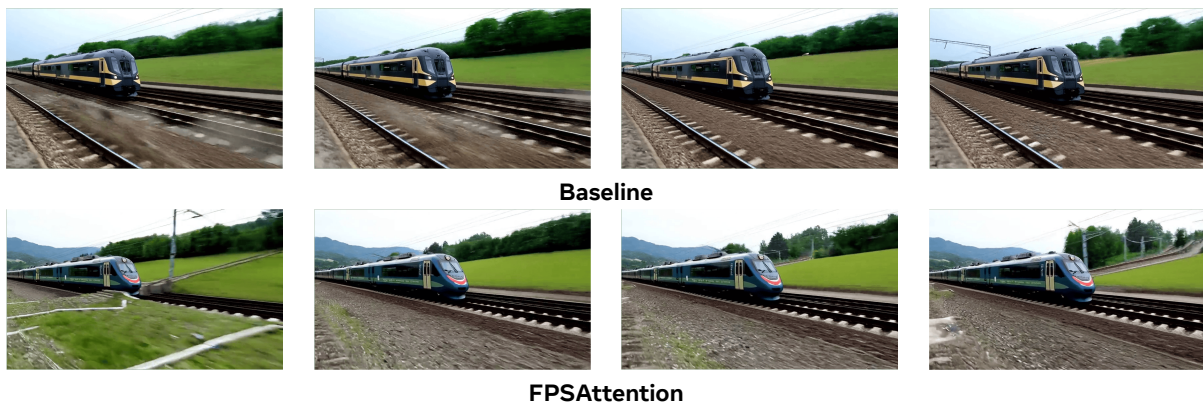


Table 15 Qualitative comparison on the rock group. Prompt: ‘A tranquil tableau of at the edge of the Arabian Desert, the ancient city of Petra beckoned with its enigmatic rock-carved façades’. Top: Baseline; Bottom: FPSAttention.

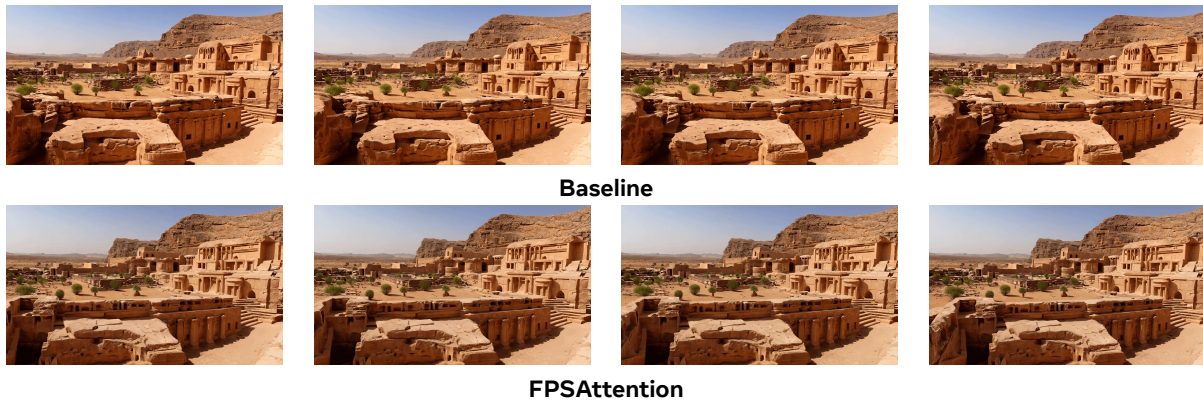


Table 16 Qualitative comparison on the nursery group. Prompt: ‘Nursery’. Top: Baseline; Bottom: FPSAttention.

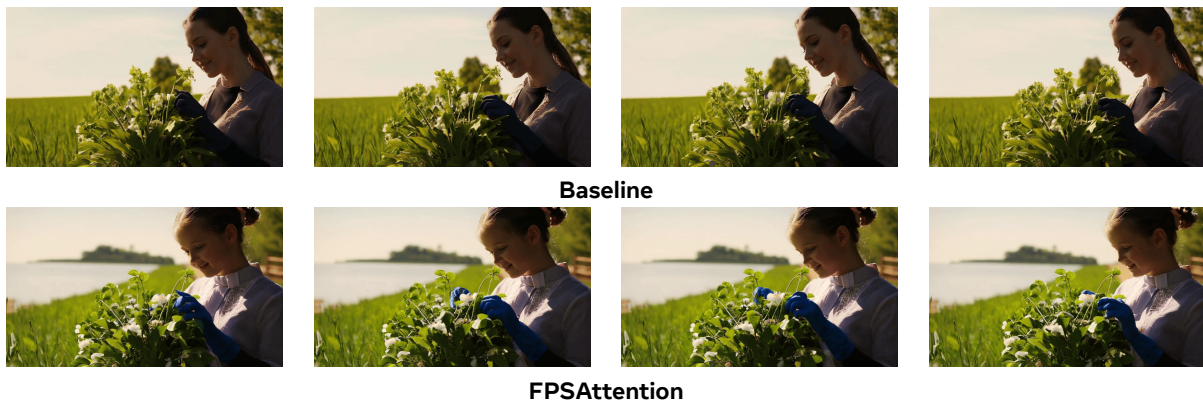


Table 17 Qualitative comparison on the snow group. Prompt: ‘Snow rocky mountains peaks canyon. snow blanketed rocky mountains surround and shadow deep canyons. The canyons twist and bend through the high elevat’. Top: Baseline; Bottom: FPSAttention.

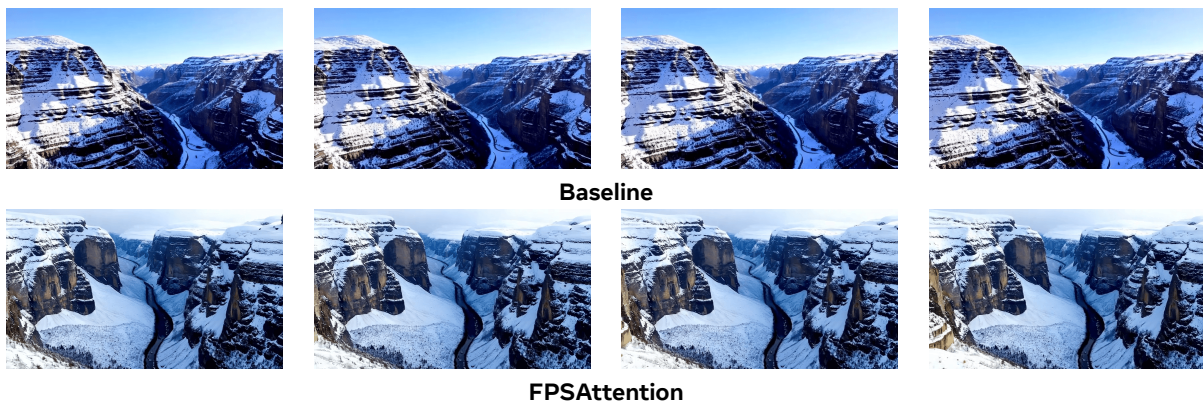


Table 18 Qualitative comparison on the book group. Prompt: ‘A person is reading book’. Top: Baseline; Bottom: FPSAttention.

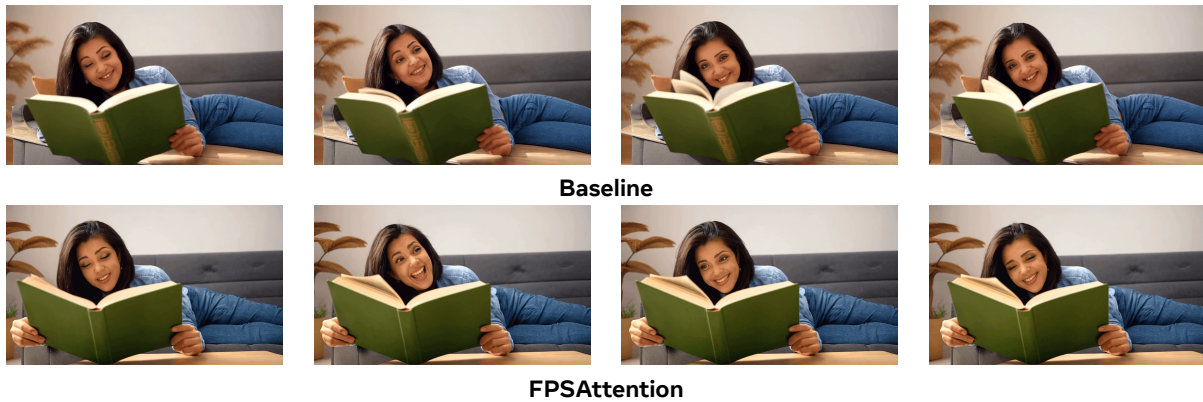


Table 19 Qualitative comparison on the space group. Prompt: ‘An astronaut flying in space’. Top: Baseline; Bottom: FPSAttention.

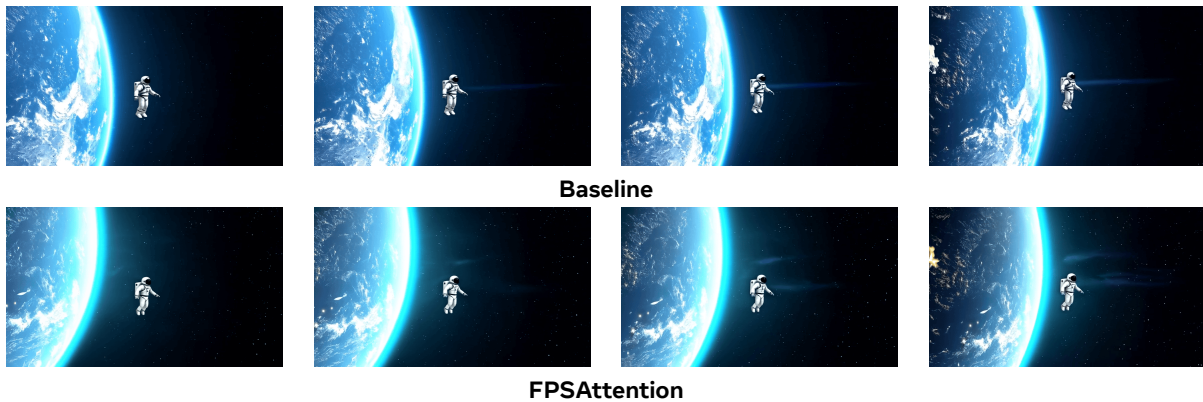
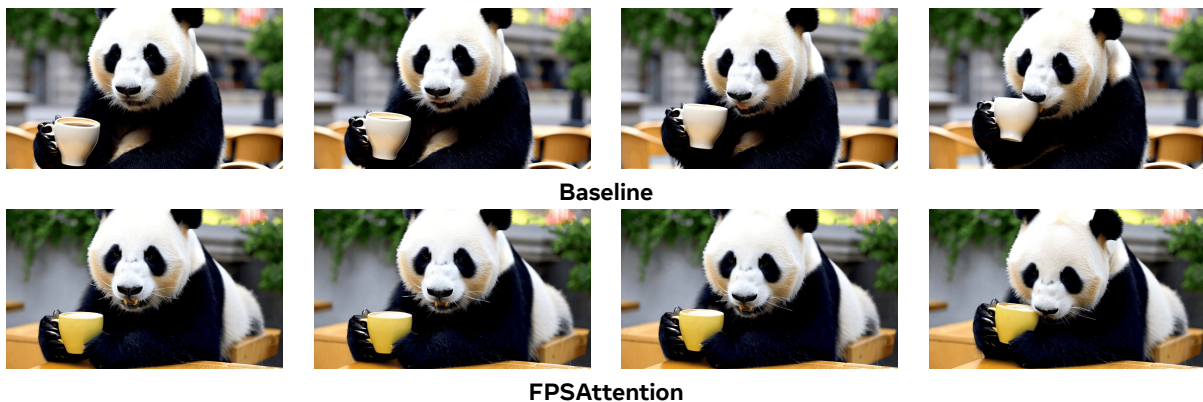


Table 20 Qualitative comparison on the panda group. Prompt: ‘A panda drinking coffee in a cafe in Paris’. Top: Baseline; Bottom: FPSAttention.



References

- [1] Andreas Blattmann, Robin Rombach, Huan Ling, Tim Dockhorn, Seung Wook Kim, Sanja Fidler, and Karsten Kreis. Align your latents: High-resolution video synthesis with latent diffusion models. In *Proceedings of the IEEE/CVF conference on computer vision and pattern recognition*, pages 22563–22575, 2023.
- [2] Jintao Chen, Chendong Xiang, Haofeng Huang, Jia Wei, Haocheng Xi, Jun Zhu, and Jianfei Chen. Ditfastattn: Attention compression for diffusion transformer models. In *Advances in Neural Information Processing Systems (NeurIPS)*, 2024.
- [3] T. Zhao, X. Ning, T. Fang, E. Liu, G. Huang, Z. Lin, S. Yan, G. Dai, and Y. Wang, “Mixdq: Memory-efficient few-step text-to-image diffusion models with metric-decoupled mixed precision quantization,” in *European Conference on Computer Vision*, 2024, pp. 285–302, Springer.
- [4] Lei Chen, Yuan Meng, Chen Tang, Xinzhu Ma, Jingyan Jiang, Xin Wang, Zhi Wang, and Wenwu Zhu. Q-dit: Accurate post-training quantization for diffusion transformers. *Proceedings of the IEEE/CVF Conference on Computer Vision and Pattern Recognition (CVPR)*, 2025.
- [5] Tri Dao. Flashattention-2: Faster attention with better parallelism and work partitioning. *arXiv preprint arXiv:2307.08691*, 2023.
- [6] Tri Dao, Dan Fu, Stefano Ermon, Atri Rudra, and Christopher Ré. Flashattention: Fast and memory-efficient exact attention with io-awareness. *Advances in neural information processing systems*, 35:16344–16359, 2022.
- [7] Prafulla Dhariwal and Alexander Nichol. Diffusion models beat gans on image synthesis. *Advances in neural information processing systems*, 34:8780–8794, 2021.
- [8] Zihan Ding, Chi Jin, Difan Liu, Haitian Zheng, Krishna Kumar Singh, Qiang Zhang, Yan Kang, Zhe Lin, and Yuchen Liu. Dollar: Few-step video generation via distillation and latent reward optimization. *arXiv preprint arXiv:2412.15689*, 2024.
- [9] Juechu Dong, Boyuan Feng, Driss Guessous, Yanbo Liang, and Horace He. Flex attention: A programming model for generating optimized attention kernels. *Proceedings of Machine Learning and Systems*, 2025.
- [10] Patrick Esser, Sumith Kulal, Andreas Blattmann, Rahim Entezari, Jonas Müller, Harry Saini, Yam Levi, Dominik Lorenz, Axel Sauer, Frederic Boesel, et al. Scaling rectified flow transformers for high-resolution image synthesis. In *ICML*, 2024.
- [11] Yefei He, Luping Liu, Jing Liu, Weijia Wu, Hong Zhou, and Bohan Zhuang. Ptqd: Accurate post-training quantization for diffusion models. *Advances in neural information processing systems*, 2023.
- [12] Jonathan Ho, Ajay Jain, and Pieter Abbeel. Denoising diffusion probabilistic models. In *Advances in Neural Information Processing Systems*, volume 33, pages 6840–6851, 2020.
- [13] Alain Hore and Djemel Ziou. Image quality metrics: Psnr vs. ssim. In *2010 20th international conference on pattern recognition*, pages 2366–2369. IEEE, 2010.
- [14] Haocheng Huang, Jiaxin Chen, Jinyang Guo, Ruiyi Zhan, and Yunhong Wang. Tcaq-dm: Timestep-channel adaptive quantization for diffusion models. In *Proceedings of the AAAI Conference on Artificial Intelligence*, number 16, pages 17404–17412, 2025.
- [15] Haocheng Huang, Jiaxin Chen, Jinyang Guo, Ruiyi Zhan, and Yunhong Wang. Tcaq-dm: Timestep-channel adaptive quantization for diffusion models. In *Proceedings of the AAAI Conference on Artificial Intelligence*, volume 39, pages 17404–17412, 2025.
- [16] Yushi Huang, Ruihao Gong, Jing Liu, Tianlong Chen, and Xianglong Liu. Tfmq-dm: Temporal feature maintenance quantization for diffusion models. In *Proceedings of the IEEE/CVF Conference on Computer Vision and Pattern Recognition (CVPR)*, pages 7362–7371, June 2024.

- [17] Ziqi Huang, Yinan He, Jiashuo Yu, Fan Zhang, Chenyang Si, Yuming Jiang, Yuanhan Zhang, Tianxing Wu, Qingyang Jin, Nattapol Chanpaisit, et al. Vbench: Comprehensive benchmark suite for video generative models. In *Proceedings of the IEEE/CVF Conference on Computer Vision and Pattern Recognition*, pages 21807–21818, 2024.
- [18] Weijie Kong, Qi Tian, Zijian Zhang, Rox Min, Zuozhuo Dai, Jin Zhou, Jiangfeng Xiong, Xin Li, Bo Wu, Jianwei Zhang, et al. Hunyuanvideo: A systematic framework for large video generative models. *arXiv preprint arXiv:2412.03603*, 2024.
- [19] Andrey Kuzmin, Mart Van Baalen, Yuwei Ren, Markus Nagel, Jorn Peters, and Tijmen Blankevoort. Fp8 quantization: The power of the exponent. *Advances in Neural Information Processing Systems*, 35:14651–14662, 2022.
- [20] Muiyang Li, Tianle Cai, Jiaxin Cao, Qinsheng Zhang, Han Cai, Junjie Bai, Yangqing Jia, Kai Li, and Song Han. Distrifusion: Distributed parallel inference for high-resolution diffusion models. In *Proceedings of the IEEE/CVF Conference on Computer Vision and Pattern Recognition*, pages 7183–7193, 2024.
- [21] Muiyang Li, Yujun Lin, Zhekai Zhang, Tianle Cai, Xiuyu Li, Junxian Guo, Enze Xie, Chenlin Meng, Jun-Yan Zhu, and Song Han. Svdquant: Absorbing outliers by low-rank components for 4-bit diffusion models. In *The Thirteenth International Conference on Learning Representations*, 2025.
- [22] Zefan Li et al. Cogvideox: Text-to-video diffusion models with an expert pipeline. *arXiv preprint arXiv:2408.06072*, 2024.
- [23] Haoyu Lu, Guoxing Yang, Nanyi Fei, Yuqi Huo, Zhiwu Lu, Ping Luo, and Mingyu Ding. Vdt: General-purpose video diffusion transformers via mask modeling. *International Conference on Learning Representations*, 2023.
- [24] Xin Ma, Yaohui Wang, Gengyun Jia, Xinyuan Chen, Ziwei Liu, Yuan-Fang Li, Cunjian Chen, and Yu Qiao. Latte: Latent diffusion transformer for video generation. *Transactions on Machine Learning Research*, 2025.
- [25] Xinyin Ma, Gongfan Fang, and Xinchao Wang. Deepcache: Accelerating diffusion models for free. In *Proceedings of the IEEE/CVF conference on computer vision and pattern recognition*, pages 15762–15772, 2024.
- [26] Laura Manduchi, Kushagra Pandey, Clara Meister, Robert Bamler, Ryan Cotterell, Sina Däubener, Sophie Fellenz, Asja Fischer, Thomas Gärtner, Matthias Kirchler, et al. On the challenges and opportunities in generative ai. *arXiv preprint arXiv:2403.00025*, 2024.
- [27] Paulius Micikevicius, Dusan Stosic, Neil Burgess, Marius Cornea, Pradeep Dubey, Richard Grisenthwaite, Sangwon Ha, Alexander Heinecke, Patrick Judd, John Kamalu, et al. Fp8 formats for deep learning. *arXiv preprint arXiv:2209.05433*, 2022.
- [28] Beatrice Alessandra Motetti, Matteo Risso, Alessio Burrello, Enrico Macii, Massimo Poncino, and Daniele Jahier Pagliari. Joint pruning and channel-wise mixed-precision quantization for efficient deep neural networks. *IEEE Transactions on Computers*, 2024.
- [29] William Peebles and Saining Xie. Scalable diffusion models with transformers. In *Proceedings of the IEEE/CVF international conference on computer vision*, pages 4195–4205, 2023.
- [30] Tim Salimans and Jonathan Ho. Progressive distillation for fast sampling of diffusion models. *arXiv preprint arXiv:2202.00512*, 2022.
- [31] Jay Shah, Ganesh Bikshandi, Ying Zhang, Vijay Thakkar, Pradeep Ramani, and Tri Dao. Flashattention-3: Fast and accurate attention with asynchrony and low-precision, 2024.
- [32] Yihua Shao, Deyang Lin, Fanhu Zeng, Minxi Yan, Muiyang Zhang, Siyu Chen, Yuxuan Fan, Ziyang Yan, Haozhe Wang, Jingcai Guo, et al. Tr-dq: Time-rotation diffusion quantization. *arXiv preprint arXiv:2503.06564*, 2025.

- [33] Haihao Shen, Naveen Mellempudi, Xin He, Qun Gao, Chang Wang, and Mengni Wang. Efficient post-training quantization with fp8 formats. *Proceedings of Machine Learning and Systems*, 6:483–498, 2024.
- [34] Hui Shen, Jingxuan Zhang, Boning Xiong, Rui Hu, Shoufa Chen, Zhongwei Wan, Xin Wang, Yu Zhang, Zixuan Gong, Guangyin Bao, et al. Efficient diffusion models: A survey. *arXiv preprint arXiv:2502.06805*, 2025.
- [35] Andy Shih, Suneel Belkhale, Stefano Ermon, Dorsa Sadigh, and Nima Anari. Parallel sampling of diffusion models. *Advances in Neural Information Processing Systems*, 36:4263–4276, 2023.
- [36] Uriel Singer, Adam Polyak, Thomas Hayes, Xi Yin, Jie An, Songyang Zhang, Qiyuan Hu, Harry Yang, Oron Ashual, Oran Gafni, et al. Make-a-video: Text-to-video generation without text-video data. *arXiv preprint arXiv:2209.14792*, 2022.
- [37] Ashish Vaswani, Noam Shazeer, Niki Parmar, Jakob Uszkoreit, Llion Jones, Aidan N Gomez, Łukasz Kaiser, and Illia Polosukhin. Attention is all you need. *Advances in neural information processing systems*, 30, 2017.
- [38] Team Wan, Ang Wang, Baole Ai, Bin Wen, Chaojie Mao, Chen-Wei Xie, Di Chen, Feiwu Yu, Haiming Zhao, Jianxiao Yang, Jianyuan Zeng, Jiayu Wang, Jingfeng Zhang, Jingren Zhou, Jinkai Wang, Jixuan Chen, Kai Zhu, Kang Zhao, Keyu Yan, Lianghua Huang, Mengyang Feng, Ningyi Zhang, Pandeng Li, Pingyu Wu, Ruihang Chu, Ruili Feng, Shiwei Zhang, Siyang Sun, Tao Fang, Tianxing Wang, Tianyi Gui, Tingyu Weng, Tong Shen, Wei Lin, Wei Wang, Wei Wang, Wenmeng Zhou, Wenten Wang, Wenting Shen, Wenyan Yu, Xianzhong Shi, Xiaoming Huang, Xin Xu, Yan Kou, Yangyu Lv, Yifei Li, Yijing Liu, Yiming Wang, Yingya Zhang, Yitong Huang, Yong Li, You Wu, Yu Liu, Yulin Pan, Yun Zheng, Yuntao Hong, Yupeng Shi, Yutong Feng, Zeyinzi Jiang, Zhen Han, Zhi-Fan Wu, and Ziyu Liu. Wan: Open and advanced large-scale video generative models, 2025.
- [39] Ang Wang, Baole Ai, Bin Wen, Chaojie Mao, Chen-Wei Xie, Di Chen, Feiwu Yu, Haiming Zhao, Jianxiao Yang, Jianyuan Zeng, et al. Wan: Open and advanced large-scale video generative models. *arXiv preprint arXiv:2503.20314*, 2025.
- [40] Changyuan Wang, Ziwei Wang, Xiuwei Xu, Yansong Tang, Jie Zhou, and Jiwen Lu. Towards accurate post-training quantization for diffusion models. In *Proceedings of the IEEE/CVF Conference on Computer Vision and Pattern Recognition*, pages 16026–16035, 2024.
- [41] Wei Wang, Yifan Zhu, Yicong Li, and Xu Yan. Controllable Generation in Diffusion Models: A Survey. *Journal of Computer Science and Technology*, 39(3):601–626, 2024.
- [42] Xiaolong Wang, Zhijian He, and Xiaojiang Peng. Artificial-intelligence-generated content with diffusion models: A literature review. *Mathematics*, 12(7):977, 2024.
- [43] Zhou Wang, A.C. Bovik, H.R. Sheikh, and E.P. Simoncelli. Image quality assessment: from error visibility to structural similarity. *IEEE Transactions on Image Processing*, 13(4):600–612, 2004.
- [44] Junyi Wu, Haoxuan Wang, Yuzhang Shang, Mubarak Shah, and Yan Yan. Ptq4dit: Post-training quantization for diffusion transformers. In *Advances in neural information processing systems*, 2024.
- [45] Haocheng Xi, Shuo Yang, Yilong Zhao, Chenfeng Xu, Muyang Li, Xiuyu Li, Yujun Lin, Han Cai, Jintao Zhang, Dacheng Li, et al. Sparse videogen: Accelerating video diffusion transformers with spatial-temporal sparsity. *International Conference on Machine Learning*, 2025.
- [46] Weiying Xie, Haowei Li, Jitao Ma, Yunsong Li, Jie Lei, Donglai Liu, and Leyuan Fang. Jointsq: Joint sparsification-quantization for distributed learning. In *Proceedings of the IEEE/CVF Conference on Computer Vision and Pattern Recognition*, pages 5778–5787, 2024.
- [47] Zhen Xing, Qijun Feng, Haoran Chen, Qi Dai, Han Hu, Hang Xu, Zuxuan Wu, and Yu-Gang Jiang. A survey on video diffusion models. *ACM Computing Surveys*, 57(2):1–42, 2024.
- [48] Sanghyun Yi, Qingfeng Liu, and Mostafa El-Khamy. Hardware-friendly static quantization method for video diffusion transformers. *arXiv preprint arXiv:2502.15077*, 2025.

- [49] Tianwei Yin, Michaël Gharbi, Richard Zhang, Eli Shechtman, Fredo Durand, William T Freeman, and Taesung Park. One-step diffusion with distribution matching distillation. In *Proceedings of the IEEE/CVF conference on computer vision and pattern recognition*, pages 6613–6623, 2024.
- [50] Jingyang Yuan, Huazuo Gao, Damai Dai, Junyu Luo, Liang Zhao, Zhengyan Zhang, Zhenda Xie, YX Wei, Lean Wang, Zhiping Xiao, et al. Native sparse attention: Hardware-aligned and natively trainable sparse attention. *arXiv preprint arXiv:2502.11089*, 2025.
- [51] Jintao Zhang, Haofeng Huang, Penge Zhang, Jia Wei, Jun Zhu, and Jianfei Chen. Sageattention2: Efficient attention with thorough outlier smoothing and per-thread int4 quantization. In *International Conference on Machine Learning (ICML)*, 2025.
- [52] Jintao Zhang, Jia Wei, Penge Zhang, Jun Zhu, and Jianfei Chen. Sageattention: Accurate 8-bit attention for plug-and-play inference acceleration. In *International Conference on Learning Representations (ICLR)*, 2025.
- [53] Jintao Zhang, Chendong Xiang, Haofeng Huang, Jia Wei, Haocheng Xi, Jun Zhu, and Jianfei Chen. Spargeattn: Accurate sparse attention accelerating any model inference. In *International Conference on Machine Learning (ICML)*, 2025.
- [54] Peiyuan Zhang, Yongqi Chen, Runlong Su, Hangliang Ding, Ion Stoica, Zhenghong Liu, and Hao Zhang. Fast video generation with sliding tile attention. *arXiv preprint arXiv:2502.04507*, 2025.
- [55] Richard Zhang, Phillip Isola, Alexei A Efros, Eli Shechtman, and Oliver Wang. The unreasonable effectiveness of deep features as a perceptual metric. In *Proceedings of the IEEE conference on computer vision and pattern recognition*, pages 586–595, 2018.
- [56] Tianchen Zhao, Tongcheng Fang, Haofeng Huang, Enshu Liu, Rui Wan, Widyadewi Soedarmadji, Shiyao Li, Zinan Lin, Guohao Dai, Shengen Yan, et al. Vidit-q: Efficient and accurate quantization of diffusion transformers for image and video generation. In *International Conference on Learning Representations*, 2025.
- [57] Xuanlei Zhao, Xiaolong Jin, Kai Wang, and Yang You. Real-time video generation with pyramid attention broadcast. In *International Conference on Learning Representations*, 2025.